# Coupling heat transfer and large eddy simulation for combustion instability prediction in a swirl burner

Christian Kraus*, Laurent Selle, Thierry Poinsot

*Institut de Mécanique des Fluides de Toulouse (IMFT), Université de Toulouse, CNRS-INPT-UPS, Toulouse, France*

## ABSTRACT

Large eddy simulations (LES) of combustion instabilities are often performed with simplified thermal wall boundary conditions, typically adiabatic walls. However, wall temperatures directly affect the gas temperatures and therefore the sound speed field. They also control the flame itself, its stabilization characteristics and its response to acoustic waves, changing the flame transfer functions (FTFs) of many combustion chambers. This paper presents an example of LES of turbulent flames fully coupled to a heat conduction solver providing the temperature in the combustor walls. LES results obtained with the fully coupled approach are compared to experimental data and to LES performed with adiabatic walls for a swirled turbulent methane/air burner installed at Engler-Bunte-Institute, Karlsruhe Institute of Technology and German Aerospace Center (DLR) in Stuttgart. Results show that the fully coupled approach provides reasonable wall temperature estimations and that heat conduction in the combustor walls strongly affects both the mean state and the unstable modes of the combustor. The unstable thermoacoustic mode observed experimentally at 750 Hz is captured accurately by the coupled simulation but not by the adiabatic one, suggesting that coupling LES with heat conduction solvers within combustor walls may be necessary in other configurations in order to capture flame dynamics.

## 1. Introduction

Heat transfer plays an important role in most power-generating systems using combustion, e.g., in gas turbines, aero engines and rocket engines. The presence of one or multiple flames leads to high temperature gradients in the system. Depending on the application, heat transfer is considered as a desired or an undesired effect. In heating units it is obviously necessary to fulfill the purpose of the machine. On the contrary, it leads to several design challenges in combustion chambers of gas turbines. Turbine blades and combustion chamber walls need to be cooled in order to withstand hot gases. This does not only raise challenges for the design of the solid parts inside the gas turbine, but also for computational fluid dynamics (CFD) when simulating the reactive flow in the combustion chambers. Boundary conditions have to be defined in a way that heat transfer processes between flow and solid parts and their impact on the temperature field inside the combustor are adequately modeled, since the temperature directly affects the flow conditions and the chemical reactions inside the combustion chamber. Advanced CFD methods like large eddy simulation (LES) combined with sophisticated flame models or direct numeri-

cal simulation (DNS) with detailed chemical mechanisms only produce accurate results when the wall temperatures in the combustion chamber are known with reasonable precision, which is rarely the case. The problem also applies to the prediction of combustion instabilities, as the acoustic behavior of combustor components is determined by the sound speed field and the geometry; flame dynamics are usually heavily influenced by changes in temperature.

There are numerous experimental and numerical studies illustrating the significant influence of heat transfer on flame dynamics and combustion instabilities. Duchaine et al. [1] demonstrated in their sensitivity study of the flame transfer function (FTF) of a laminar premixed flame that the duct wall temperature has a strong impact on the velocity field and the local flame speed, which leads to uncertainties in the prediction of the phase of the FTF. Kaess et al. [2] investigated the influence of the thermal wall boundary condition on the FTF of a laminar premixed flame with DNS. Their results showed that the flame anchoring position as well as the FTF were significantly altered when changing the adiabatic boundary condition to an isothermal boundary condition. The FTF of the case with the isothermal wall shows a better agreement with the experimentally obtained FTF. Mejia et al. [3] observed a strong influence of the burner rim temperature on the combustion dynamics of a laminar premixed flame: an unstable mode could be triggered by switching on the cooling system of the burner rim. They

* Corresponding author.
   *E-mail address:* kraus@cerfacs.fr (C. Kraus).

explained this behavior with altered flame foot dynamics [4,5], which lead in turn to changes in the FTF. The study of Hong et al. [6] showed that heat transfer is not only controlled by temperature gradients, but also by the physical properties of the solid combustor parts. Replacing the stainless steel flame holder with one made of ceramics inhibited or delayed the onset of a combustion stability. The authors conclude that the wall thermal conductivity influences the flame speed near the flame holder, which leads to a distinct dynamic behavior of the flame for each flame holder material. Lohrmann and Büchner [7] investigated the influence of the preheat temperature on the FTF of a turbulent swirl-stabilized premixed flame. The delay of the flame response decreased with increasing preheat temperature, which they explained by an increase in the turbulent flame speed that shifts the main reaction zone to an upstream location.

Despite the fact that the influence of wall temperatures on flame dynamics has been observed in many studies, a major hurdle remains: wall temperatures are very difficult to determine in most combustors. As a consequence, heat transfer is neglected in many CFD simulations. Walls are often treated as adiabatic, or at best isothermal but with a guessed temperature. Nevertheless, numerical simulations are often able to capture the right thermoacoustic mode in an unstable laboratory-scale combustor, even when heat transfer is neglected. Differences in frequency or amplitude may occur when the temperature field and the FTF in the simulation only partially match those in the experiment, but the simulation can usually be used for further investigation of the thermoacoustic mode. There are numerous studies of combustion instabilities that illustrate that LES with adiabatic walls can show a reasonable agreement with experiments: the study on a lean-premixed swirl combustor by Huang et al. [8], the LES-studies on the PRECCIN-STA configuration [9–11], the massively parallel LES of a realistic helicopter combustion chamber by Wolf et al. [12], LESs of model rocket combustors (Garby et al. [13], Urbano et al. [14]) or the LES-studies of bluff-body stabilized flames by Li et al. [15] and Ghani et al. [16].

However, as illustrated by the simulation of the LIMOUSINE burner performed by Shahi et al. [17], taking into account the heat transfer between the flow and the solid parts of the combustion chamber can significantly increase the accuracy of the results. Another example is the study by Kraus et al. [18], who compared an adiabatic LES and an LES with basic modeling of heat transfer between fluid and solid material. Both LESs show the same mode structure, but taking into account heat transfer effects leads to a higher accuracy in terms of frequency.

To summarize the state of the art in this field, LES of combustors can be classified into four categories, depending on their thermal boundary conditions on walls:

- Type 1: Adiabatic walls: the majority of recent LESs simply consider the walls to be adiabatic [8–16,19–22].
- Type 2: Imposed wall temperatures [23–27]: when experimental data on wall temperatures is available, imposing them as boundary conditions for LES may be a solution. Note that this can be a dangerous methodology: imposing a high local wall temperature may for example, force the flame to anchor at this point, diminishing the predictive quality of the method by forcing the solution artificially. Moreover, limited experimental information is usually available on wall temperatures, which are measured only at a few points. The introduction of diagnostics such as laser induced phosphorescence [27,28] in laboratory-scale experiments may help in certain cases as it can provide a full temperature field on combustor walls. However, in most real engines, detailed wall temperature information is simply not available, making type 2 LES unpractical in industrial cases.

- Type 3: A simple method to account for wall heat transfer is to write a Robin condition [29] on walls linking the wall temperature $T_w$ to the local heat flux $\Phi$ through a heat resistance $R$ and a cooling temperature $T_\infty$: $\Phi = (T_w - T_\infty)/R$ where $R$ is roughly evaluated from the combustor wall characteristics [18,30–32]. This is a cheap method to account for dual heat transfer between reacting flow and conduction through walls.
- Type 4: Fully coupled LES/heat conduction solver in the combustor walls: the whole combustor solid structure is also meshed and the temperature within the solid structure is computed by a solver coupled with the LES flow solver [17,33–35].

Most LES are of type 1 because the combustion community does not consider the problem of heat conduction through walls as an interesting one compared to the other challenges found in turbulent flames. However, the benefits of going to a type 4 simulation are obvious as shown by Berger et al. [35]: the LES becomes fully predictive and does not rely on any ad hoc evaluation of wall temperatures in the solid. For a cooled chamber, the only input data is the cooling water temperature and the convection coefficient in the cooling passages between water and combustor walls. On the long term, it is clear that the high precision of LES will require a corresponding high precision for wall temperatures and therefore type 4 simulations. This is true not only for the mean flow characteristics but also for pollutants and for flame dynamics or flame stabilization: Miguel-Brebion et al. [33], e.g., show that flames stabilized behind uncooled or cooled cylinders exhibit totally different shapes, which are well captured when a type 4 simulation is performed. The results of these studies show that not only heat losses have to be considered, but also heat transfer inside the solid parts of combustors, as it can have a strong impact on the temperature field inside the combustion chamber and therefore on combustion. Especially the adequate modeling of internal heat transfer inside the combustor is almost impossible without applying fully coupled simulations of type 4, since temperatures on internal walls in combustors are in most cases unknown.

The present paper shows that a type 4 LES for a full combustion chamber is possible today even in a complex swirl burner and that it allows significant improvements in the description of the flame dynamics, especially to capture self-excited modes: taking into account internal heat transfer from the combustion chamber to other combustor parts can strongly affect thermoacoustics and flame dynamics.

The coupled LES is performed with a fully compressible solver for reacting flows [30,36–38] and a heat conduction solver in the combustor walls coupled to the LES solver with the OpenPalm tool [39] (www.cerfacs.fr/globc/PALM-WEB/). The results of the coupled LES are compared to the results of an adiabatic LES, which is performed with the same numerical setup but with adiabatic walls.

The experiment is briefly presented in Section 2, followed by the description of the numerical setup in Section 3. The impact of accounting for heat transfer in the coupled simulation on the temperature field is depicted in Section 4. Mean velocities and acoustic spectra obtained in the experiment are compared to the LES data. Possible reasons for the differences in combustion dynamics observed between adiabatic and coupled LES are discussed. The paper is concluded by a summary of the main observations and results.

## 2. Experimental setup

The KIT-Burner is described in detail in [40] and [41], therefore only a brief presentation of its main features is given here.

Identical versions of the burner are installed at two locations: one at Engler-Bunte-Institute, Combustion Technology at Karlsruhe Institute of Technology and the other at DLR (German Aerospace Center) in Stuttgart. It is operated under atmospheric conditions
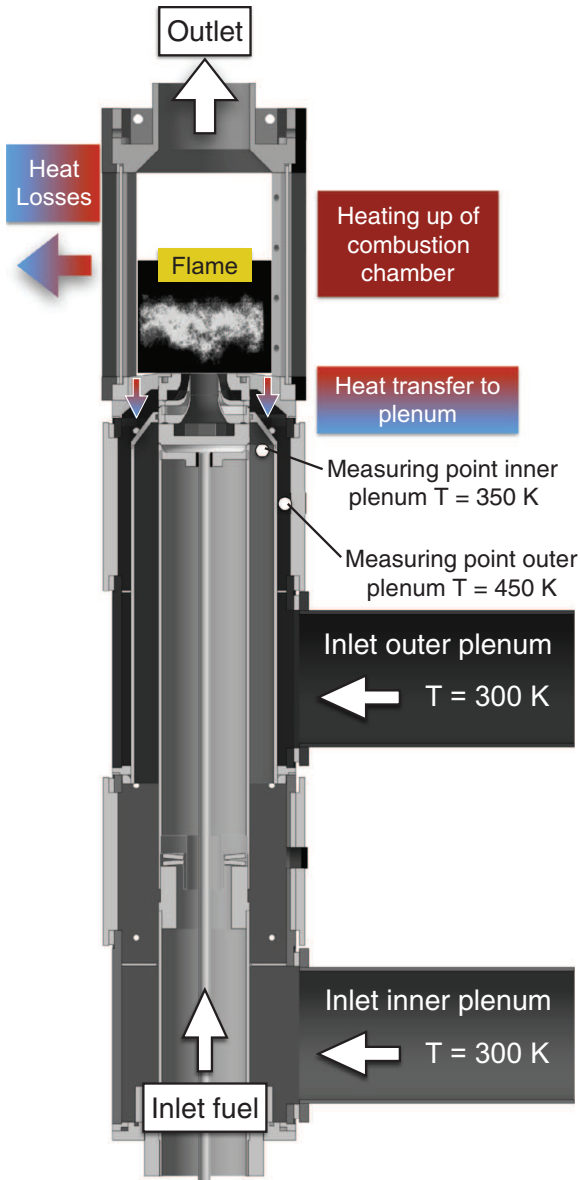
**Fig. 1.** KIT-Burner with two separated air inlets for the double-concentric swirl nozzle. During operation the hot gases in the combustion chamber heat up the combustion chamber. Due to heat conduction inside the solid parts heat is transferred to the plenum and heats up the fresh gases.

with no preheating of the fresh gases. A sketch of the combustor is shown in Fig. 1. It is approximately 1 m long and the cross section of the combustion chamber is of rectangular shape, with a width of 89 mm and a height of 114 mm. The first section of the outlet is of conical shape and the second section has a constant diameter of 50 mm. For optical access, the combustion chamber is equipped with quartz windows. Microphones measure pressure oscillations inside the combustion chamber and the plenums.

The combustor has two air inlets, one for each swirler, and the mass flow in each swirler can be controlled individually. Therefore the nozzle can be operated with different air split ratios $L = \dot{m}_{OTS}/\dot{m}_{IS}$ (OTS = outer swirler, IS = inner swirler). Perforated plates are installed inside both the inner and the outer plenum to homogenize the flow before it enters the swirlers.

The fuel is either methane (DLR) or natural gas (>90% $CH_4$, KIT) and is injected through 60 circumferentially distributed holes (hole diameter 0.5 mm) into the air flow of the inner swirler, which re-

sults in partially premixed flames. The influence of the fuel composition on the amplitudes and frequencies of the unstable combustor modes is very limited, typically 1.5% for the frequency.

No additional cooling is applied to the combustor, neither to the combustion chamber nor the plenum. Air and fuel are injected at ambient temperature, i.e. around 300 K. At the given operating conditions (thermal power $P_{th} = 30$ kW, global equivalence ratio $\phi = 0.85$, $L = 1.6$), the heating-up of the combustion chamber and the heat transferred into the plenum by heat conduction in the solid material lead to flow temperatures (measured in the experiment) of around 450 K in the outer plenum and 350 K in the inner plenum.

## 3. Numerical setup

### 3.1. Fluid solver—AVBP

The flow simulations are performed with the solver AVBP, which is developed by CERFACS and IFPEN. AVBP is a finite volume solver with a cell-vertex approach [30,37]. It solves the fully compressible Navier–Stokes equations on unstructured grids. The Lax–Wendroff scheme is used as numerical method, which is of second order in time and space; the CFL-Number is set to 0.9. The unresolved turbulent scales are modeled with a filtered Smagorinsky subgrid scale model [42].

Reaction kinetics are described with the BFER two-step mechanism for methane [10], which is valid over a wide range of equivalence ratios:

$$CH_4 + 1.5O_2 \rightarrow CO + 2H_2O,$$

$$CO + 0.5O_2 \leftrightarrow CO_2.$$
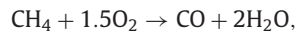
The dynamic thickened flame model (DTF) [43–47] is used to model turbulence/flame interaction. The DTF model allows to thicken the reaction zones of premixed flames by dividing the chemical pre-exponential constants by a factor $F$ and multiplying diffusion terms by $F$. This is done in a limited spatial zone identified by a flame sensor [44]. The flame thickness being increased by a factor $F$, an efficiency function is introduced to account for the subgrid scale wrinkling [43,48].

The geometry used in the simulations comprises the combustion chamber and the whole plenum. A hybrid mesh was generated with the commercial software CENTAUR, which has around $13.6 \times 10^6$ cells and was used in both adiabatic and coupled LES. One layer of prism cells is used at the wall (required by the wall model [49,50]) while all other cells are tetrahedral.

Two different LESs are compared in this work:

- A type 1 approach where heat transfer between the flow and the combustor parts is completely neglected and all walls are considered as adiabatic.

- A type 4 approach where heat transfer between the flow and the solid combustor parts as well as heat conduction inside the solid parts are taken into account.

### 3.2. Solid heat conduction solver AVTP and coupling strategy

The simulation of heat transfer in the solid combustor parts is performed with the AVTP code [51,52], which solves the time dependent energy equation:

$$\rho_s C_s \frac{\partial T}{\partial t} = \frac{\partial \dot{q}_i}{\partial x_i},$$

where $T$ is the temperature, $\rho_s$ the density and $C_s$ the heat capacity of the solid material, whereas $\dot{q}_i$ denotes conduction heat flux.
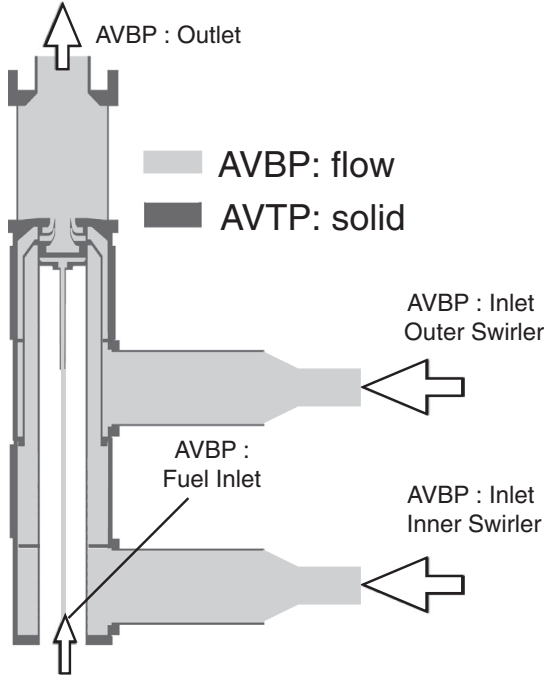
Fig. 2. Geometries used for the fluid solver AVBP and the solid solver AVTP.



Fig. 3. Modulus and phase of the reflection coefficient $R$ of the combustion chamber outlet: ——— impedance model of Levine and Schwinger [57], ‐‐‐‐ NSCBC formulation used in the LESs with $K = 30000$ s$^{-1}$.

Heat diffusion is modeled with Fourier's law:

$$\dot{q}_i = -\lambda_s \frac{\partial T}{\partial x_i},$$

with $\lambda_s$ being the heat conductivity of the solid material. The differences in heat capacity and heat conductivity of the different materials used for the construction of the combustor as well as the influence of temperature on heat capacity and conductivity are taken into account. Heat transfer via radiation is not included in the current simulations.

The 3D mesh for the solid domain contains $4.5 \times 10^6$ tetrahedral cells. The geometry comprises the solid material of the combustion chamber and the plenum as well as parts of the inlets for air and fuel, as depicted in Fig. 2. For spatial discretization, a second-order Galerkin diffusion scheme is applied and time integration is performed with an implicit first-order Euler scheme.

AVBP and AVTP are coupled using the OpenPalm software [39]. Thermal equilibrium in the experiment is reached after about 30 min. This is far beyond computational resources for the LES solver (time step: $\sim 10^{-7}$ s). In order to speed up the convergence of the temperature field inside the solid domain, the fluid and solid solvers are de-synchronized in time. The solid solver operates with larger time steps ($\sim 10^{-4}$ s) and during the transient period data is exchanged between the solvers every 50 iterations of the fluid solver. This approach is equivalent to decreasing the heat capacity of the solid material. After the solid has reached thermal equilibrium, the time step of the solid solver and exchange rate are synchronized with the time advancement of the fluid solver.

Compared to the computationally expensive fluid solver, the additional computational cost due to the solid solver is not significant [53]. The increased computational cost of the coupled simulation is merely caused by the additional simulation time needed to reach thermal equilibrium in the solid domain. This leads to a computational cost of around 200000 CPU hours compared to around 100000 CPU hours for the adiabatic simulation on 1056 Intel 12-Core E5-2690 V3 processors (supercomputer OCCIGEN) and 1248 Intel(r) 10 core IVYBRIDGE 2.8 Ghz processors (supercomputer EOS). It also shows that type 4 LES will become standard in the future, since they introduce acceptable additional cost.
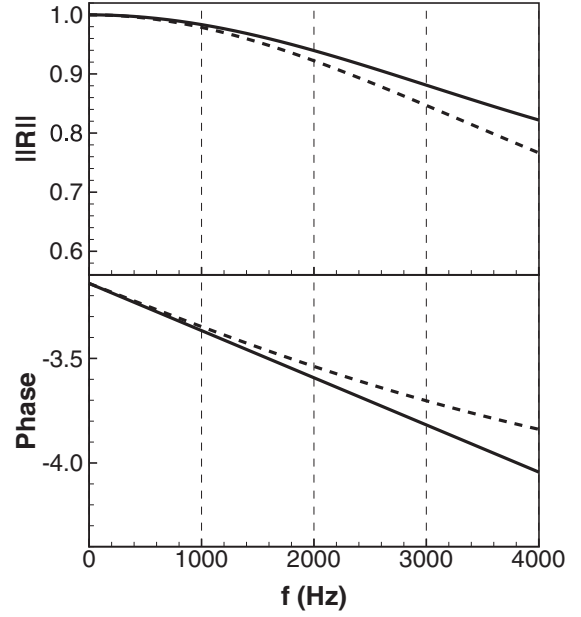
### 3.3. Boundary conditions—coupled and adiabatic LES

The inlet and outlet boundary conditions in AVBP are handled with the NSCBC approach (Navier–Stokes-characteristic-boundary-conditions [54,55]). With the NSCBC approach, the ingoing wave amplitude $\mathcal{L}^-$ at the combustor outlet is written:

$$\mathcal{L}^- = K(p - p_\infty)$$

where $p$ is the local pressure, $p_\infty$ the pressure at infinity and $K$ the relax parameter of the boundary condition. The magnitude $||R||$ and the phase $\phi$ of the NSCBC boundary condition $\phi$ may be expressed by [56]:

$$||R|| = \frac{1}{\sqrt{1 + (\frac{2\omega}{K})^2}} \quad \text{and} \quad \phi = -\pi - \arctan\left(\frac{2\omega}{K}\right),$$

with the angular frequency $\omega$. The relax parameter $K$ can be tuned to match the impedance of the combustion chamber outlet: the acoustic behavior of the outlet of the combustion chamber is that of an open-end pipe, which can be described by the impedance model by Levine and Schwinger [57]. The value of $K$ of the NSCBC boundary condition at the combustion chamber outlet in the LESs is adapted to match the acoustic impedance given by the model of Levine and Schwinger. With $K = 30000$ s$^{-1}$, the NSCBC impedance matches the model impedance very well in the relevant frequency range of $f = 0$–2000 Hz (Fig. 3).

In order to predict heat transfer between the walls and the fluid with reasonable accuracy, the thermal boundary layer has to be resolved or modeled. On the walls of the outlet section of the combustion chamber, no-slip boundary conditions are imposed and the grid resolution in the region results in values of $y+$ of around 2–5. This also allows to reproduce the acoustic behavior of the outlet section of the combustion chamber, which has a strong influence on the frequency of the unstable mode. Wall models [49,50] for momentum and heat are applied on the other combustion chamber chamber walls as well as on the walls in the swirlers and in the fuel plenum, as resolving the thermal boundary layer everywhere in the domain would have been computationally too costly.

The flow inside the air plenums is considered as mostly laminar, since the Reynolds numbers are below Re = 2000; therefore
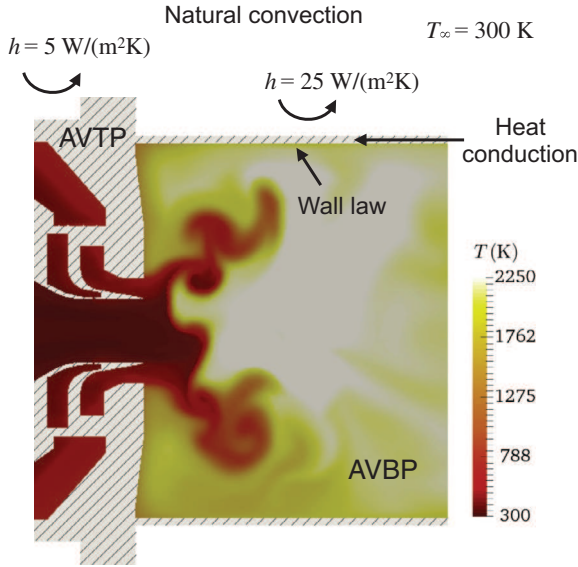
**Fig. 4.** Thermal boundary conditions and modeling of heat transfer in the coupled LES. The color field corresponds to an instantaneous field of temperature. (For interpretation of the references to colour in this figure legend, the reader is referred to the web version of this article.)

no-slip boundary conditions are imposed inside the plenum. The heat conduction inside the solid material leads to a heating up of the perforated plates, which in turn results in a temperature increase of the air flow passing through the holes. In order to account for this effect, the flow inside the holes of the perforated plates is also computed.

On the coupled boundary surfaces, the heat flux on the wall calculated by AVBP is imposed as boundary condition for AVTP and the temperature at the wall calculated by AVTP is imposed as wall temperature for AVBP. All walls in the fluid domain are coupled. The heat transfer on the external surface of the walls of the solid domain is modeled under the assumption of natural convection, with heat transfer coefficients of $h = 5$ W m$^{-2}$ K$^{-1}$ for the plenum walls and $h = 25$ W m$^{-2}$ K$^{-1}$ for the combustion chamber walls, assuming a cooling temperature of the surrounding air of $T_\infty = 300$ K (Fig. 4).

## 4. Results

### 4.1. Preheating of fresh gases due to heat transfer in the coupled simulation

The preheating of the fresh gases observed during the experiment can also be observed in the coupled simulation. Figure 5 shows the mean temperatures calculated by the coupled simulation in the flow field and the solid material. The hot gases in the combustion chamber heat the walls of the combustion chamber. This heat is conducted inside the solid material and heats up the solid material of the plenum. Near the inlets of the vanes of the outer swirler the temperature of the solid material rises to temperatures going from $T = 500$ to $700$ K.

The hot plenum walls heat the air flows in the plenum: the temperatures of the fresh gases reach values around $T = 360$ K in the inner swirler and $T = 510$ K in the outer swirler. Heat is also transferred to the nozzle and conducted to the inner plenum, which leads to a significant increase of the fuel flow temperature to around $T = 460$ K near the injection holes. Table 1 compares the mean temperatures predicted by the LES at the locations where the thermocouples are mounted in the experiment. The temperatures are very similar to those measured in the experiment, which indi-

**Table 1**
Air temperatures at measuring points in the plenums in the experiment and the coupled LES.

| Case | Outer plenum (K) | Inner plenum (K) |
|---|---|---|
| Experiment | 450 | 350 |
| Coupled LES | 443 | 344 |

cates that the heat transfer in the solid material is reasonably well reproduced.

Figure 6(a) quantifies the heat losses to the surrounding air and the internal heat transfer inside the combustor in the coupled LES in reference to heat added by the combustion process. Around 10.5% of the combustion heat is lost at the external walls. Most of it is transferred by the combustion chamber walls (10%). Around 7% of the combustion heat is transferred through the solid parts from the combustion chamber to the plenum. A small percentage is lost at the external plenum walls (0.5%), but most of it is absorbed by the fresh gases (6.5%), mostly in the outer plenum (5%).

Heat losses and especially internal heat transfer from the combustion chamber lead to a temperature field in the coupled LES which differs significantly from the one in the adiabatic LES. Figure 6(b) shows the relative temperature difference $(\bar{T}_{CP} - \bar{T}_{AD})/\bar{T}_{AD}$ on the middle plane of the domain. The highest temperatures differences are located in the outer plenum near the inlets of the swirl vanes of the outer swirler (up to 140%), whereas the heat losses in the combustion chamber result in temperature decreases of around $-18\%$ at the combustion chamber walls.

When the fluid and the solid solvers are synchronized in time, the temperatures in the solid remain almost constant. This is caused by the disparity of the heat transfer time scale and the characteristic fluid time scale. Given the high heat conductivity of the solid material, the corresponding Biot Numbers $Bi$ can be considered small ($Bi < 0.01$). Assuming a constant fluid temperature, a characteristic time scale for the heat transfer in the solid material can be estimated with [58]:

$$t_0 = \frac{m_s C_s}{hS},$$

with the surface area $S$ and the mass of the solid $m_s$. Depending on the region considered (stainless steel walls or quartz glass walls), $t_0$ varies between values of the order of $\sim 1$ s to $\sim 10$ s. Comparing $t_0$ to the characteristic time scale of the instability, the time period $T$ ($t_0 \sim 10^{-3}$ s), it can be stated that transient wall heating does not play an important role in the current case. Therefore it can be assumed that a similar temperature field of the flow field could have been achieved by using isothermal boundary conditions and imposing the right wall temperatures. However, estimating the right wall temperatures and imposing a similar, complex 2D temperature distribution, as it is achieved by the coupled simulation, is very complicated, if not impossible in the current case.

The impact of the differences in temperature between coupled and adiabatic LES on the mean flow fields, the thermoacoustic behavior and the flames shapes in both LESs are discussed in the following sections.

### 4.2. Mean flow fields—PIV vs. LES

The PIV measurements were performed by DLR Stuttgart [18]. Figure 7 shows the mean velocity profiles and Fig. 8 the RMS velocities for the axial, radial and azimuthal components at different axial coordinates in the combustion chamber. Velocities are normalized by the bulk velocities measured or calculated at the outlets of the swirlers. To calculate the bulk velocity in the experiment, the profile for the axial velocity is considered to be axisymmetric. Table 2 lists the bulk velocity for each case. The bulk
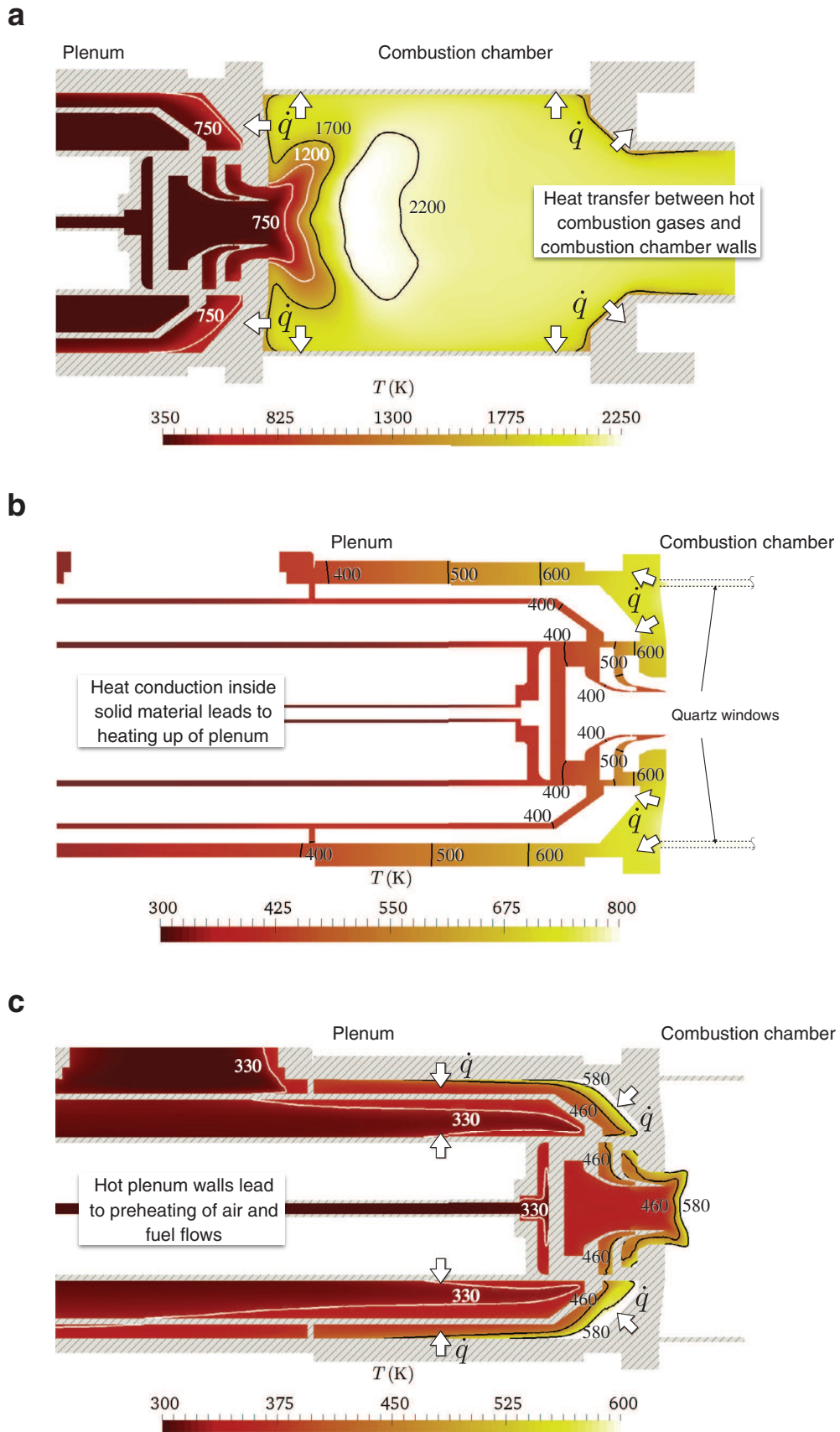
**Fig. 5.** Preheating of the fresh gases induced by heat transfer between flow and solid material and heat conduction inside the solid domain. (a) Flow temperature in the combustion chamber and near the nozzle outlet, (b) temperature in the solid, (c) flow temperature in the preheating zone.
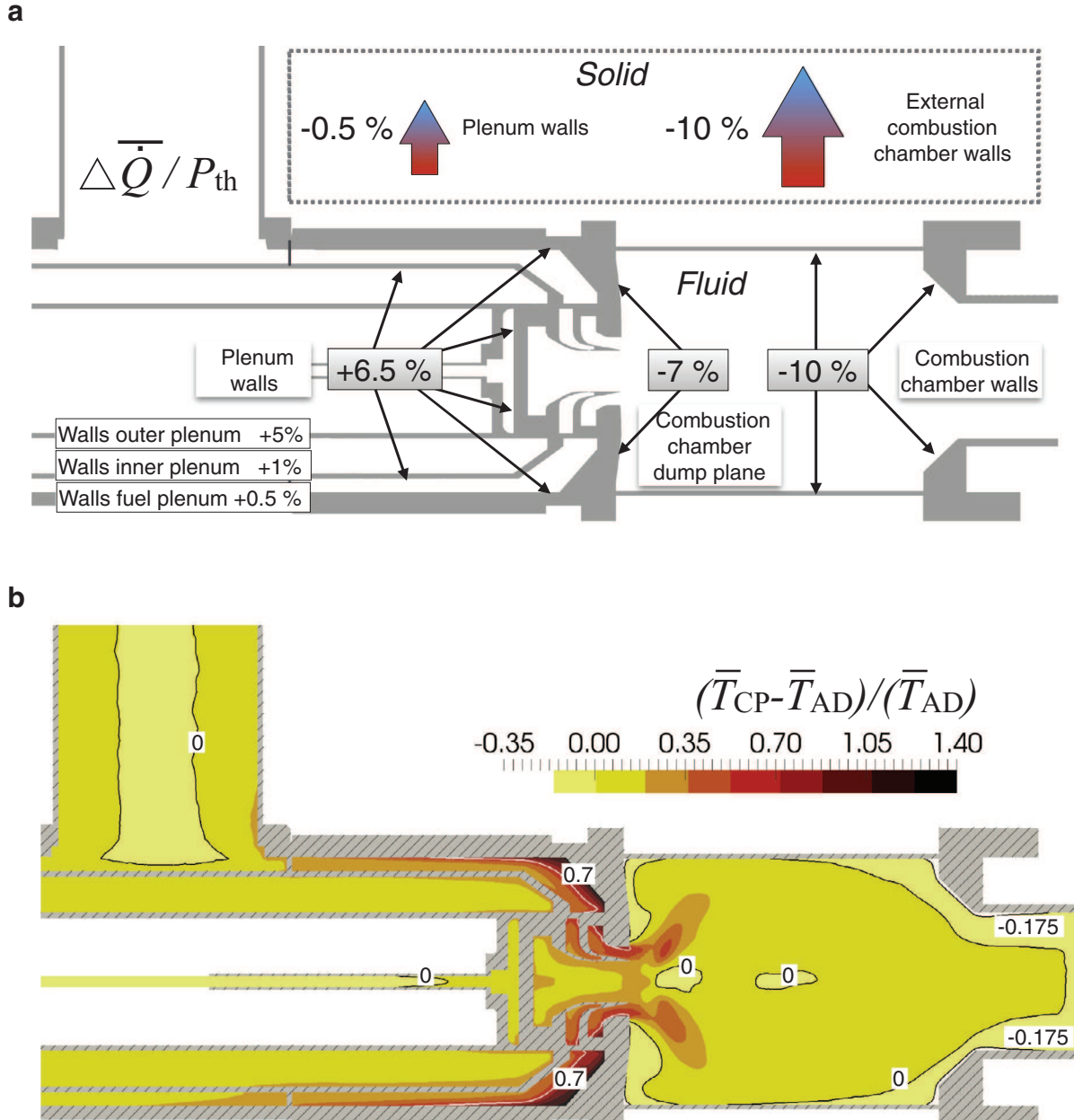
**Fig. 6.** (a) Heat losses and internal heat transfer in the coupled LES, the heat fluxes are normalized with the thermal power of the flame ($\Delta\dot{\overline{Q}}/P_{\text{th}}$), (b) relative mean temperature difference between the coupled and the adiabatic LES ($\overline{T}_{CP} - \overline{T}_{AD})/\overline{T}_{AD}$ on the middle plane of the combustor.

**Table 2**
Mean bulk velocities in the PIV, the adiabatic and the coupled LES at the nozzle outlet.

| Case | Bulk velocity (m s$^{-1}$) |
|------|---------------------------|
| Experiment | 31.4 |
| Adiabatic LES | 23.1 |
| Coupled LES | 33.5 |

velocity in the adiabatic LES is lower than in the experiment, whereas the coupled LES shows only a slight overestimation. This is clearly due to the preheating of the fresh gases found in the experiment and the coupled LES. The increased fresh gas temperature leads to a density decrease and therefore to an increase of the bulk velocity.

Both LESs show a reasonable agreement with PIV because velocities are only marginally sensitive to temperature changes. On the other hand, when comparing the overall shape of the profiles, discrepancies can be observed between the adiabatic LES and the PIV for $x/d = 0.2$ (Fig. 7, left images). PIV and coupled LES exhibit maximum mean axial velocities near the outlet of the outer swirler, whereas they are located closer to the burner axis in the adiabatic LES. In general, the adiabatic LES overestimates the normalized velocity components close to the burner axis for $x/d = 0.2$ and $x/d = 0.4$. This can be explained by the preheating of the fresh gases in the experiment and the coupled LES, which causes higher temperatures of the air flow in the outer swirler than in the inner swirler, which in turn leads to higher velocities in the outer swirler. Since the adiabatic LES does not account for heat transfer processes, it cannot reproduce this behavior.

Further downstream, the mean flow fields of the LESs are more similar and show both an overestimation of the angle of the swirl flow. The differences in swirl angle can be caused by the
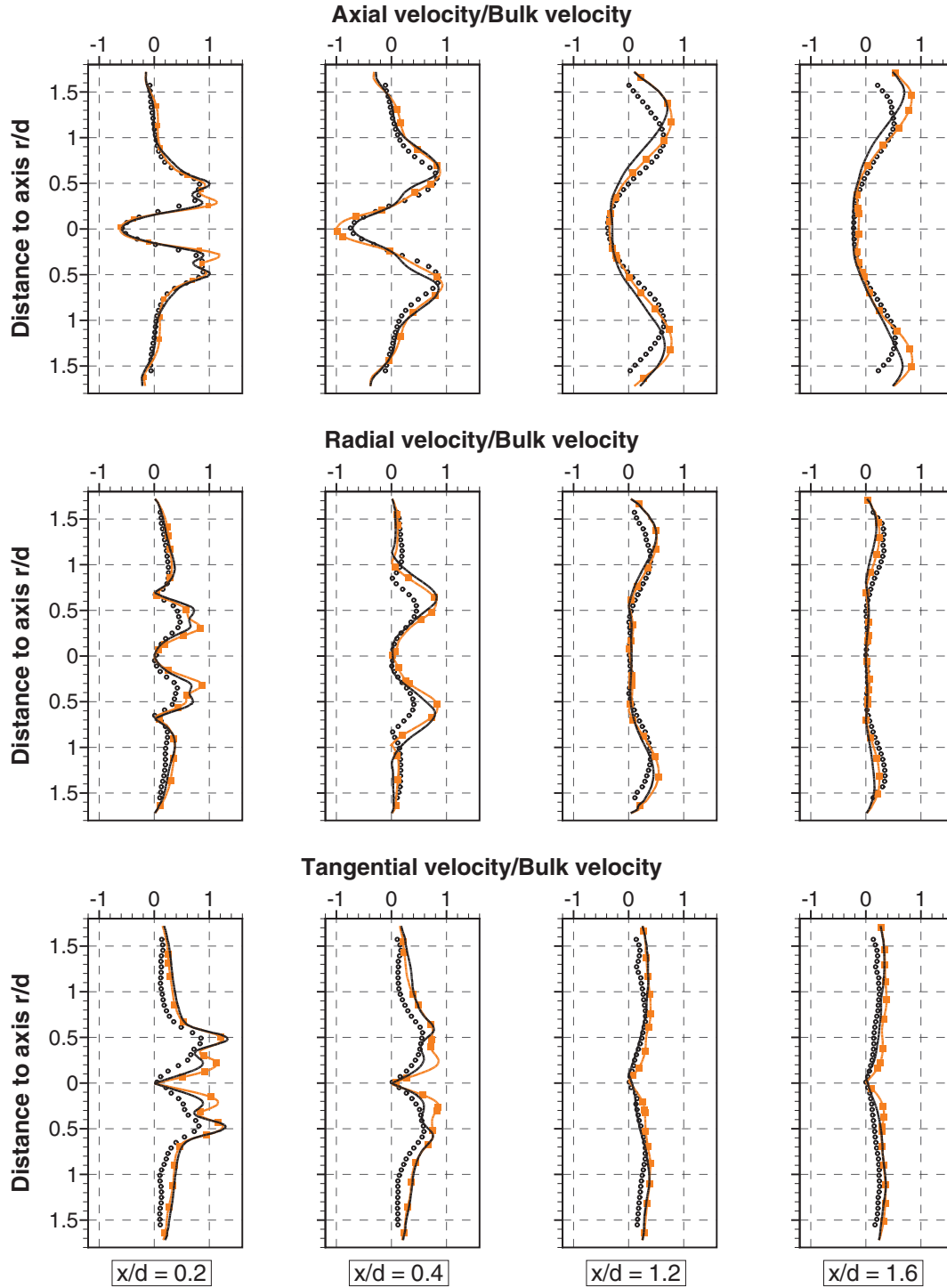
## Axial velocity/Bulk velocity

## Radial velocity/Bulk velocity

## Tangential velocity/Bulk velocity

x/d = 0.2  x/d = 0.4  x/d = 1.2  x/d = 1.6

**Fig. 7.** Mean normalized velocities in the PIV (●), the adiabatic LES (—■—) and the coupled LES (——).

significantly higher velocity fluctuations in the LESs (Fig. 8), as amplitude and frequency of velocity oscillations can influence the mean flow field in a swirl flow [59–61]. The increased RMS velocities in both LES are related to the pressure spectra, which are further discussed in Section 4.3.

### 4.3. Pressure spectra

As discussed in Section 4.2, both LESs show reasonable agreement with the experiment regarding the mean flow fields. How-

ever, this is not the case for the acoustics and the unstable mode (Fig. 9). The pressure spectra in the combustion chamber illustrate that both LESs show a combustion instability, but the frequency of the unstable mode in the adiabatic LES ($f = 864$ Hz) is significantly higher than in the experiment ($f = 750$ Hz) and the mode amplitude is significantly lower. The frequency in the coupled LES agrees perfectly with the experiment ($f = 750$ Hz) and the mode amplitude in the combustion chamber is comparable to the one in the experiment. The frequency resolution of the pressure spectra of the LES is about $\Delta f = 8$ Hz.
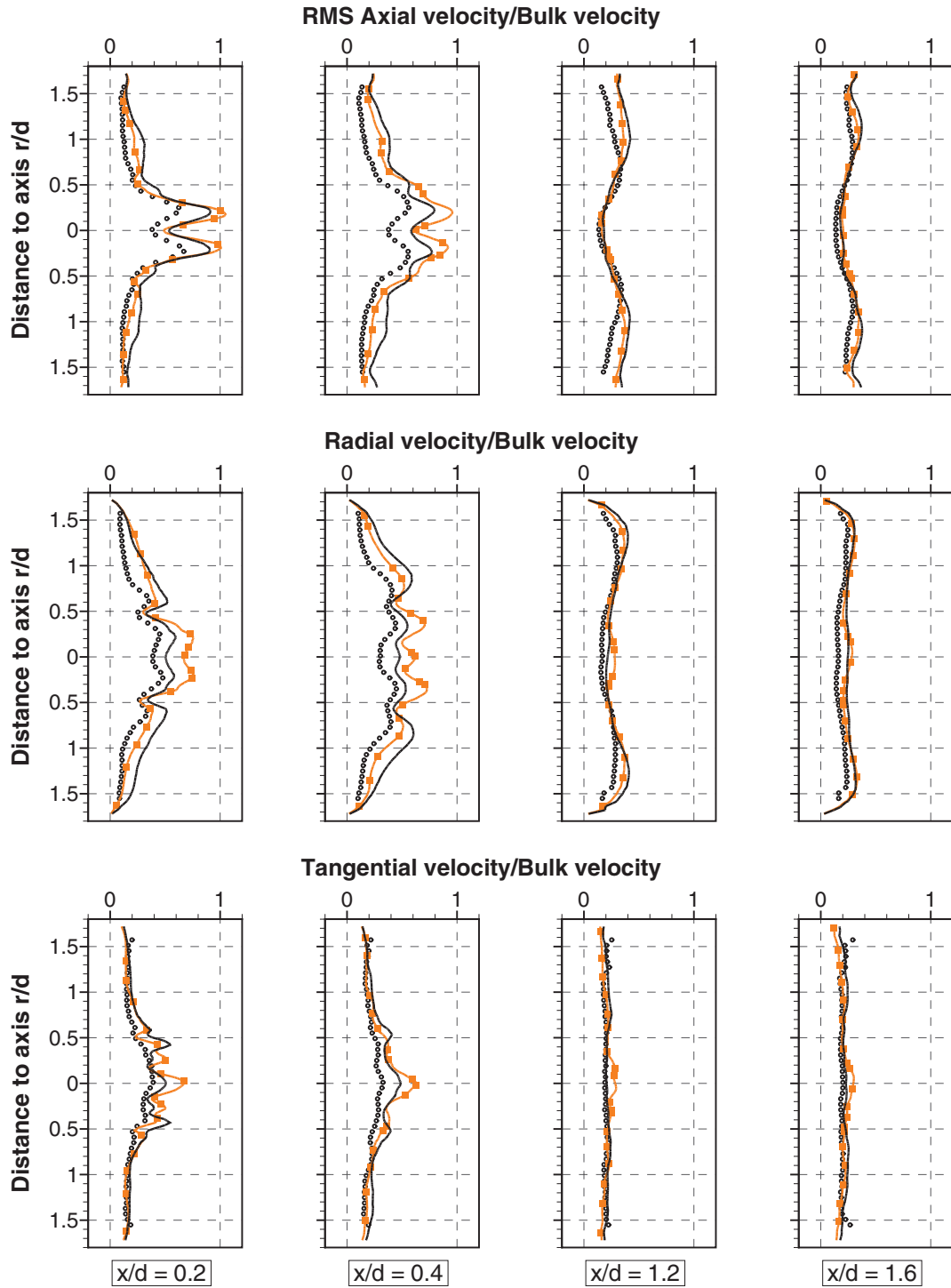
**Fig. 8.** Mean normalized RMS of the velocities in the PIV (●), the adiabatic LES (──■──) and the coupled LES (────).

Differences between the spectra of both LESs and the experiment are found in the low-frequency range, especially the inner plenum at frequencies around $f = 500$ Hz. This indicates that the acoustic impedances of the inner plenum are not perfectly reproduced in the simulations. Possible reasons for this are the walls, which are perfectly reflective in the LESs, which is not the case in the experiment; additional sources of uncertainties are the impedances of the perforated plates in the LESs. Even though the flow in the holes is calculated, small differences in the hole geometries between the experiment and the LES, due to e.g., the

manufacturing process of the holes, may affect the hole impedance [62,63] and lead to discrepancies between simulation and experiment. The mesh resolution in and around the holes may also not be sufficient to perfectly reproduce the acoustic behavior of the perforated plates in the LESs.

Although the difference in accuracy regarding the simulation of the instability between the coupled and the adiabatic LES is very significant, it should be noted that the results of the LESs are also influenced by other factors (chemistry model, numerical accuracy, subgrid models, boundary conditions). It is therefore
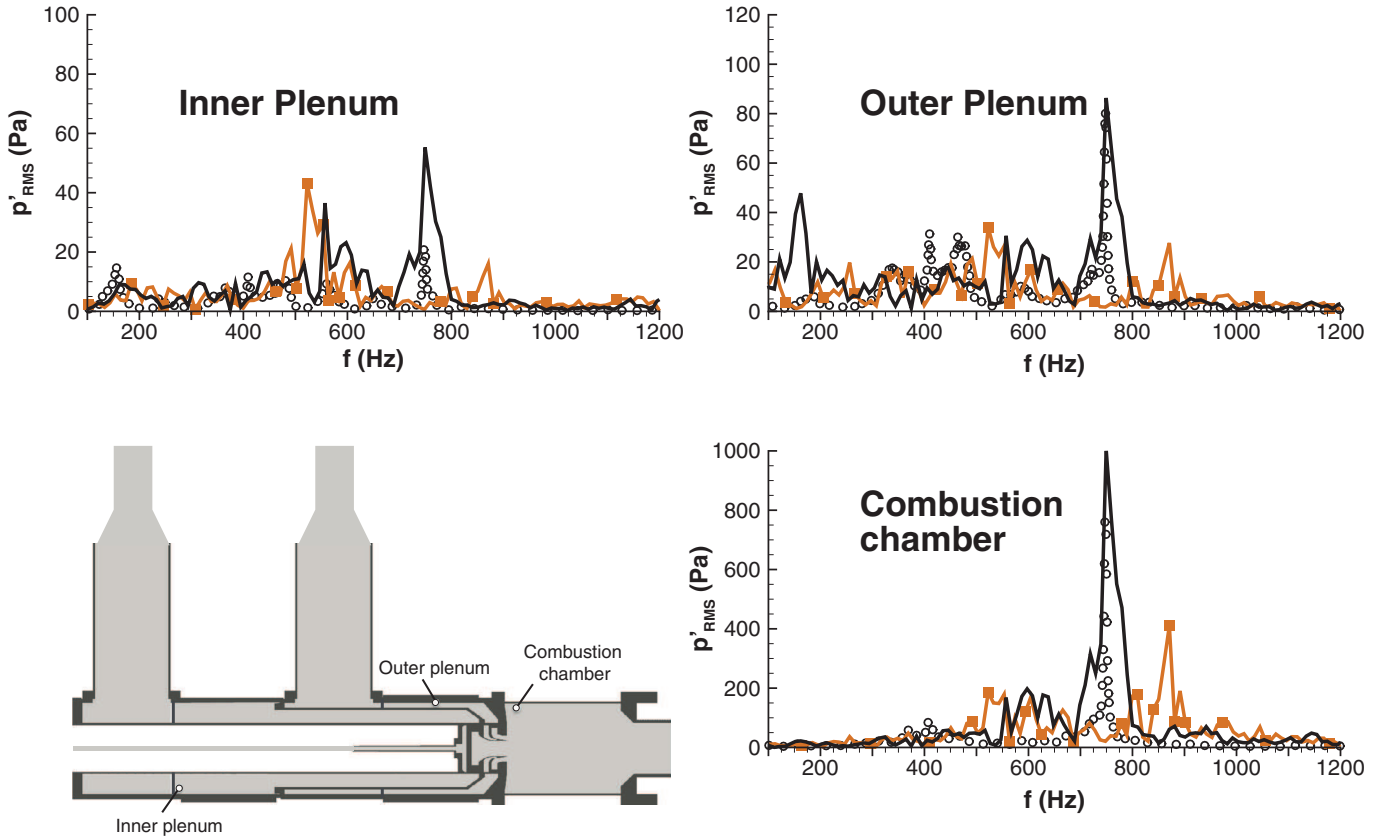
Fig. 9. Pressure spectra in the PIV (●), the adiabatic LES (──■──) and the coupled LES (────).

possible that choosing a different chemical mechanism [64], increasing the mesh resolution, applying a different model for the turbulent flame [65,66] or using different acoustic boundary conditions would have an impact on the flow field and the flame structure and influence acoustic spectra and combustion dynamics. Accounting for heat radiation could also influence amplitude and frequency of the unstable mode in the LES. Berger et al. [35] show that radiative fluxes can be of the same order of magnitude as the convective fluxes. However, they also observed that accounting for heat radiation had only a limited impact on the flow. While investigating the sensitivity of the LESs to different numerical models represents an significant topic, it is beyond the scope of this work. In any case, the present results strongly suggest that taking into account heat transfer within the combustor walls has a strong impact on the thermoacoustic modes in the combustor. In order to further investigate why this is the case, the mode shapes of the unstable modes, the flame shapes and the distributions of the mean Rayleigh index in both LES cases are discussed in the following section.

### 4.4. Unstable mode structures, flame shapes and Rayleigh index

In order to compare the mode shapes of the main unstable modes in both LES cases, the values of the mean amplitude and phase of the pressure oscillations in the combustion chamber, the outer swirler and the outer plenum were extracted following a predefined path. Figure 10 shows the path where pressure amplitude and phase were extracted and compares the resulting mode structures in the adiabatic and the coupled LES. The mode shape in the combustion chamber does not show a significant gradient in the transverse direction: therefore, for clarity reasons, it was only extracted on the centerline. The modes shapes are similar; how-
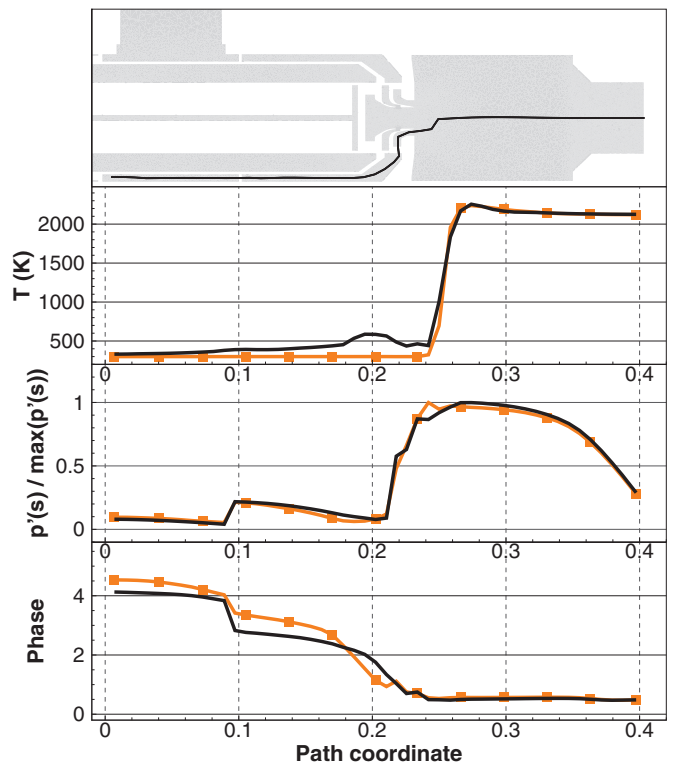


Fig. 10. Mode structures of the unstable modes in the adiabatic LES (──■──) and the coupled LES (────). The mode structures were extracted along the path depicted in the upper image.
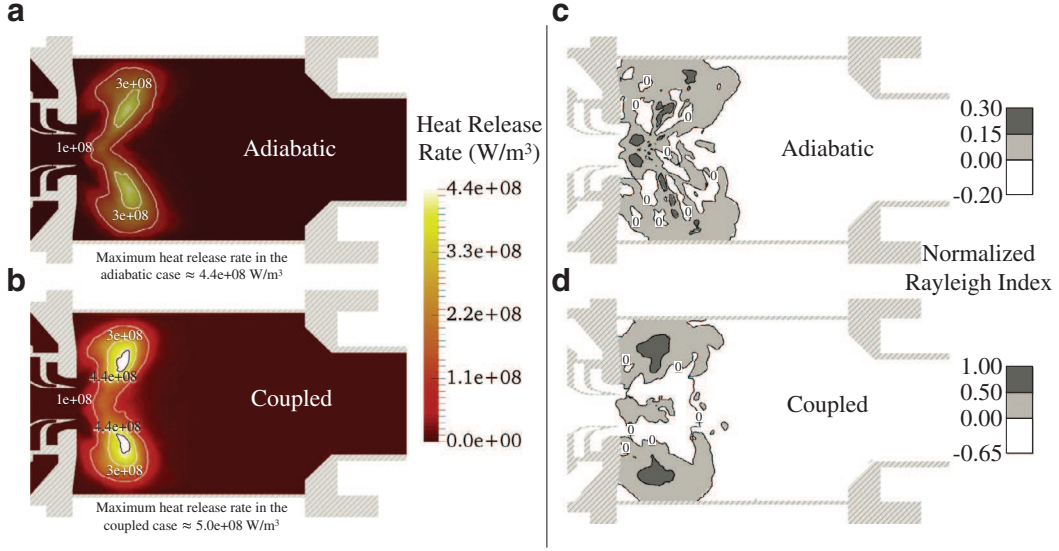
**Fig. 11.** Mean fields of heat release rate (a, b) and Rayleigh index (c, d) in the adiabatic (a, c) and the coupled LES (b, d).

ever, differences on both amplitude and phase are found inside the outer swirler and the outer plenum near the inlets of the swirler vanes. This indicates that the temperature increase in the plenum induces changes in the acoustic impedance, which in turns leads to differences in the mode shape compared to the adiabatic LES.

Figure 11 shows mean fields of heat release rate and Rayleigh indexes in both LESs, normalized by the maximum value found in both LES. The Rayleigh index (RI) is defined as:

$$RI = \frac{1}{\tau} \int_\tau \overline{p'\dot{q}'} dt,$$

where $p'$ and $\dot{q}'$ are respectively the pressure and heat release rate fluctuations and $\tau$ is the time period of the mode. It characterizes the interaction of the flame with the acoustic field: a positive RI means that the flame adds energy to the acoustic field, whereas an RI smaller than zero means that unsteady combustion damps acoustic oscillations in these regions. The preheating of the fresh gases and the subsequent increased flame speed in the coupled LES has several effects: compared to the adiabatic case, the maximum heat release is increased and the flame is more compact and located further upstream. The distributions of the Rayleigh index are also different: in the coupled case, the regions with positive and negative RIs are clearly separated and the highest RIs are found in the region with the highest heat release rate. In the adiabatic case, the zones of negative and positive RIs are rather distributed.

Consistent observations are made analyzing the axial distribution of the mean heat release rate and the RI. The main reaction zone is more compact in the coupled case and the flame is located further upstream (Fig. 12). In both LESs the mean heat release rate continuously grows and diminishes, with a maximum value at around $x/d = 0.9$ in the coupled LES and around $x/d = 1.0$ in the adiabatic LES. In the coupled LES, the axial distribution of the RI follows the shape of the mean heat release rate with a small shift in the upstream direction and reaches its maximum value at around $x/d = 0.8$. This is not the case in the adiabatic LES, where the axial distribution of the RI exhibits a different shape than the heat release distribution and reaches its maximum further downstream.

The fields of the RI represent all thermoacoustic modes in the combustor and not only the main unstable mode. A separate assessment of the RI for each mode is not available with our current database. However, it is clearly visible that the characteristics and the locations of the strongest thermoacoustic coupling are differ-
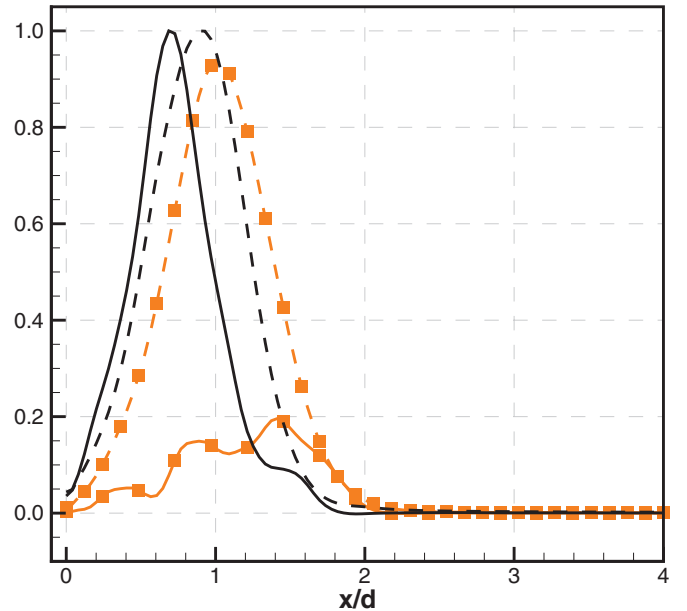


**Fig. 12.** Mean axial distributions of: the heat release rate in the adiabatic LES (--■--) and the coupled LES (----), the RI in the adiabatic LES (—■—) and the coupled LES (——).

ent in both cases. Since the distribution of the RI is not available in the experimental data, it cannot be said to what extent the coupled LES matches the thermoacoustics of the experiment. However, the fact that the very good agreement in terms of frequency and amplitude strongly suggests that the coupled LES reproduces well the combustion instability in the experiment, which illustrates the advantages of coupled simulations compared to adiabatic simulations when heat transfer has a significant impact on combustion dynamics.

## 5. Conclusions

The current paper discusses the potential of fully coupled LES/heat transfer simulation to improve the accuracy of numerical simulations for the prediction of combustion instabilities. The combustion instability in a laboratory-scale swirl burner is

computed with an adiabatic and a fully coupled LES, which accounts for heat transfer between flow and burner as well as heat conduction in the solid burner structure. The results of the LESs and their comparison with the experimental data show that although the coupled simulation does not significantly improve the prediction of the mean velocity field, it performs much better regarding the prediction of frequency and amplitude of the unstable mode. The heat conduction inside the solid structure results in a preheating of the fresh gases in the coupled LES, which influences the mode shape and alters the characteristics of the flame-acoustics coupling in comparison of the adiabatic LES.

The results strongly suggest that, in order to obtain an accurate prediction of combustion instabilities, it may be mandatory to account for heat transfer in the solid structure in combustors of complex geometry, where heat transfer has a strong impact on the flow temperature. Coupled simulations provide an excellent possibility to do this, as the full 3D distribution in the solid material can be computed, and the coupling of the fluid and the solid solver allows to impose a non-uniform, complex 2D temperature field on the wall boundaries for the fluid solver, which is impossible to obtain with non-coupled simulations.

## References

[1] F. Duchaine, F. Boudy, D. Durox, T. Poinsot, Sensitivity analysis of transfer functions of laminar flames, Combust. Flame 158 (12) (2011) 2384–2394, doi:10.1016/j.combustflame.2011.05.013.

[2] R. Kaess, W. Polifke, T. Poinsot, N. Noiray, D. Durox, T. Schuller, S. Candel, CFD-based mapping of the thermo-acoustic stability of a laminar premix burner, Proceedings of the 2008 Summer Program (2008), pp. 289–302.

[3] D. Mejia, L. Selle, R. Bazile, T. Poinsot, Wall-temperature effects on flame response to acoustic oscillations, Proc. Combust. Inst. 35 (3) (2014) 3201–3208, doi:10.1016/j.proci.2014.07.015.

[4] K.S. Kedia, H.M. Altay, A.F. Ghoniem, Impact of flame-wall interaction on premixed flame dynamics and transfer function characteristics, Proc. Combust. Inst. 33 (1) (2011) 1113–1120, doi:10.1016/j.proci.2010.06.132.

[5] A. Cuquel, D. Durox, T. Schuller, Impact of flame base dynamics on the nonlinear frequency response of conical flames, C.R. Mec. 341 (1–2) (2013) 171–180, doi:10.1016/j.crme.2012.11.004.

[6] S. Hong, S.J. Shanbhogue, K.S. Kedia, A.F. Ghoniem, Impact of the flame-holder heat-transfer characteristics on the onset of combustion instability, Combust. Sci. Technol. 185 (10) (2013) 1541–1567, doi:10.1080/00102202.2013.816575.

[7] M. Lohrmann, H. Büchner, Prediction of stability limits for LP and LPP gas turbine combustors, Combust. Sci. Technol. 177 (12) (2005) 2243–2273, doi:10.1080/00102200500241040.

[8] Y. Huang, H.-G. Sung, S.-Y. Hsieh, V. Yang, Large-Eddy simulation of combustion dynamics of lean-premixed swirl-stabilized combustor, J. Propul. Power 19 (5) (2003) 782–794, doi:10.2514/2.6194.

[9] S. Roux, G. Lartigue, T. Poinsot, U. Meier, C. Bérat, Studies of mean and unsteady flow in a swirled combustor using experiments, acoustic analysis, and large Eddy simulations, Combust. Flame 141 (1–2) (2005) 40–54, doi:10.1016/j.combustflame.2004.12.007.

[10] B. Franzelli, E. Riber, L.Y. Gicquel, T. Poinsot, Large Eddy simulation of combustion instabilities in a lean partially premixed swirled flame, Combust. Flame 159 (2) (2012) 621–637, doi:10.1016/j.combustflame.2011.08.004.

[11] P.S. Volpiani, T. Schmitt, D. Veynante, Large eddy simulation of a turbulent swirling premixed flame coupling the TFLES model with a dynamic wrinkling formulation, Combust. Flame 180 (2017) 124–135, doi:10.1016/j.combustflame.2017.02.028.

[12] P. Wolf, G. Staffelbach, L.Y. Gicquel, J.-D. Müller, T. Poinsot, Acoustic and large eddy simulation studies of azimuthal modes in annular combustion chambers, Combust. Flame 159 (11) (2012) 3398–3413, doi:10.1016/j.combustflame.2012.06.016.

[13] R. Garby, L. Selle, T. Poinsot, Large-Eddy simulation of combustion instabilities in a variable-length combustor, C.R. Mec. 341 (1–2) (2013) 220–229, doi:10.1016/j.crme.2012.10.020.

[14] A. Urbano, L. Selle, G. Staffelbach, B. Cuenot, T. Schmitt, S. Ducruix, S. Candel, Exploration of combustion instability triggering using large eddy simulation of a multiple injector liquid rocket engine, Combust. Flame 169 (2016) 129–140, doi:10.1016/j.combustflame.2016.03.020.

[15] H.-G. Li, P. Khare, H.-G. Sung, V. Yang, A large-eddy-simulation study of combustion dynamics of bluff-body stabilized flames, Combust. Sci. Technol. 188 (6) (2016) 924–952, doi:10.1080/00102202.2015.1136296.

[16] A. Ghani, T. Poinsot, L. Gicquel, G. Staffelbach, LES of longitudinal and transverse self-excited combustion instabilities in a bluff-body stabilized turbulent premixed flame, Combust. Flame 162 (11) (2015) 4075–4083, doi:10.1016/j.combustflame.2015.08.024.

[17] M. Shahi, J.B. Kok, J. Roman Casado, A.K. Pozarlik, Transient heat transfer between a turbulent lean partially premixed flame in limit cycle oscillation and the walls of a can type combustor, Appl. Therm. Eng. 81 (2015) 128–139, doi:10.1016/j.applthermaleng.2015.01.060.

[18] C. Kraus, L. Selle, T. Poinsot, C.M. Arndt, H. Bockhorn, Influence of heat transfer and material temperature on combustion instabilities in a swirl burner, J. Eng. Gas Turbines Power (2016), doi:10.1115/GT2016-56368.

[19] Y.C. See, M. Ihme, Large eddy simulation of a partially-premixed gas turbine model combustor, Proc. Combust. Inst. 35 (2) (2015) 1225–1234, doi:10.1016/j.proci.2014.08.006.

[20] V. Moureau, P. Domingo, L. Vervisch, From large-eddy simulation to direct numerical simulation of a lean premixed swirl flame: filtered laminar flame-PDF modeling, Combust. Flame 158 (7) (2011) 1340–1357, doi:10.1016/j.combustflame.2010.12.004.

[21] R. Mercier, V. Moureau, D. Veynante, B. Fiorina, LES of turbulent combustion: on the consistency between flame and flow filter scales, Proc. Combust. Inst. 35 (2) (2015) 1359–1366, doi:10.1016/j.proci.2014.05.149.

[22] G. Bulat, E. Fedina, C. Fureby, W. Meier, U. Stopper, Reacting flow in an industrial gas turbine combustor: LES and experimental analysis, Proc. Combust. Inst. 35 (3) (2015) 3175–3183, doi:10.1016/j.proci.2014.05.015.

[23] S.R. Gubba, S.S. Ibrahim, W. Malalasekera, A.R. Masri, Measurements and LES calculations of turbulent premixed flame propagation past repeated obstacles, Combust. Flame 158 (12) (2011) 2465–2481, doi:10.1016/j.combustflame.2011.05.008.

[24] P. Palies, T. Schuller, D. Durox, L.Y.M. Gicquel, S. Candel, Acoustically perturbed turbulent premixed swirling flames, Phys. Fluids 23 (3) (2011) 037101, doi:10.1063/1.3553276.

[25] H.J. Krediet, C.H. Beck, W. Krebs, S. Schimek, C.O. Paschereit, J.B.W. Kok, Identification of the flame describing function of a premixed swirl flame from LES, Combust. Sci. Technol. 184 (7–8) (2012) 888–900, doi:10.1080/00102202.2012.663981.

[26] S. Gövert, D. Mira, J.B. Kok, M. Vázquez, G. Houzeaux, Turbulent combustion modelling of a confined premixed jet flame including heat loss effects using tabulated chemistry, Appl. Energy 156 (2015) 804–815, doi:10.1016/j.apenergy.2015.06.031.

[27] R. Mercier, T.F. Guiberti, A. Chatelier, D. Durox, O. Gicquel, N. Darabiha, T. Schuller, B. Fiorina, Experimental and numerical investigation of the influence of thermal boundary conditions on premixed swirling flame stabilization, Combust. Flame 171 (2016) 42–58, doi:10.1016/j.combustflame.2016.05.006.

[28] J. Brübach, C. Pflitsch, A. Dreizler, B. Atakan, On surface temperature measurements with thermographic phosphors: a review, Prog. Energy Combust. Sci. 39 (1) (2013) 37–60, doi:10.1016/j.pecs.2012.06.001.

[29] K. Gustafson, Domain decomposition, operator trigonometry, robin condition, in: J. Mandel, F. Charbel, X.C. Cai (Eds.), Proceedings of the 10th International Conference on Domain Decomposition Methods, vol. 218, American Mathematical Society, Boulder (1998), pp. 432–437.

[30] P. Schmitt, T. Poinsot, B. Schuermans, K.P. Geigle, Large-eddy simulation and experimental study of heat transfer, nitric oxide emissions and combustion instability in a swirled turbulent high-pressure burner, J. Fluid Mech. 570 (May) (2007) 17, doi:10.1017/S0022112006003156.

[31] I. Hernández, G. Staffelbach, T. Poinsot, J.C. Román Casado, J.B. Kok, LES and acoustic analysis of thermo-acoustic instabilities in a partially premixed model combustor, C.R. Mec. 341 (1–2) (2013) 121–130, doi:10.1016/j.crme.2012.11.003.

[32] M. Bauerheim, G. Staffelbach, N.A. Worth, J.R. Dawson, L.Y.M. Gicquel, T. Poinsot, Sensitivity of LES-based harmonic flame response model for turbulent swirled flames and impact on the stability of azimuthal modes, Proc. Combust. Inst. 35 (3) (2015) 3355–3363, doi:10.1016/j.proci.2014.07.021.

[33] M. Miguel-Brebion, D. Mejia, P. Xavier, F. Duchaine, B. Bedat, L. Selle, T. Poinsot, Joint experimental and numerical study of the influence of flame holder temperature on the stabilization of a laminar methane flame on a cylinder, Combust. Flame 172 (2016) 153–161, doi:10.1016/j.combustflame.2016.06.025.

[34] A. Ghani, M. Miguel-Brebion, L. Selle, F. Duchaine, D.T. Poinsot, Effect of wall heat transfer on screech in a turbulent premixed combustor, Center for Turbulence Research Proceedings of the Summer Program (2016), pp. 133–141.

[35] S. Berger, S. Richard, F. Duchaine, G. Staffelbach, L.Y.M. Gicquel, On the sensitivity of a helicopter combustor wall temperature to convective and radiative thermal loads, Appl. Therm. Eng. 103 (2016) 1450–1459, doi:10.1016/j.applthermaleng.2016.04.054.

[36] N. Gourdain, L. Gicquel, G. Staffelbach, O. Vermorel, F. Duchaine, J.-F. Boussuge, T. Poinsot, High performance parallel computing of flows in complex geometries: II. Applications, Comput. Sci. Discovery 2 (1) (2009) 015004, doi:10.1088/1749-4699/2/1/015004.

[37] O. Colin, M. Rudgyard, Development of high-order Taylor–Galerkin schemes for LES, J. Comput. Phys. 162 (2) (2000) 338–371, doi:10.1006/jcph.2000.6538.

[38] T. Schönfeld, M. Rudgyard, Steady and unsteady flows simulations using the hybrid flow solver AVBP, AIAA J. 37 (11) (1999) 1378–1385.

[39] F. Duchaine, S. Jauré, D. Poitou, E. Quémerais, Analysis of high performance conjugate heat transfer with the OpenPALM coupler, Comput. Sci. Discovery 8 (1) (2015) 15003, doi:10.1088/1749-4699/8/1/015003.

[40] C. Kraus, S. Harth, H. Bockhorn, Experimental investigation of combustion instabilities in lean swirl-stabilized partially-premixed flames in single- and multiple-burner setup, Int. J. Spray Combust. Dyn. 0 (0) (2016) 1–23, doi:10.1177/1756827715627064.

[41] C.M. Arndt, M. Severin, C. Dem, M. Stöhr, A.M. Steinberg, W. Meier, Experimental analysis of thermo-acoustic instabilities in a generic gas turbine combustor by phase-correlated PIV, chemiluminescence, and laser Raman scattering measurements, Exp. Fluids 56 (4) (2015) 1–23, doi:10.1007/s00348-015-1929-3.

[42] F. Ducros, P. Comte, M. Lesieur, Large-eddy simulation of transition to turbulence in a boundary layer developing spatially over a flat plate, J. Fluid Mech. 326 (1996) 1–36, doi:10.1017/S0022112096008221.

[43] O. Colin, F. Ducros, D. Veynante, T. Poinsot, A thickened flame model for large eddy simulations of turbulent premixed combustion, Phys. Fluids 12 (7) (2000) 1843–1863, doi:10.1063/1.870436.

[44] J.P. Legier, T. Poinsot, D. Veynante, Dynamically thickened flame LES model for premixed and non-premixed turbulent combustion, Proceedings of the Summer Program (2000), pp. 157–168.

[45] C. Martin, L. Benoit, F. Nicoud, T. Poinsot, Y. Sommerer, Large-Eddy simulation and acoustic analysis of a swirled staged turbulent combustor, AIAA J. 44 (4) (2006) 741–750, doi:10.2514/1.14689.

[46] M. Boileau, G. Staffelbach, B. Cuenot, T. Poinsot, C. Berat, LES of an ignition sequence in a gas turbine engine, Combust. Flame 154 (1–2) (2008) 2–22, doi:10.1016/j.combustflame.2008.02.006.

[47] P. Schmitt, T. Poinsot, B. Schuermans, K.P. Geigle, Large-Eddy simulation and experimental study of heat transfer, nitric oxide emissions and combustion instability in a swirled turbulent high-pressure burner, J. Fluid Mech. 570 (2007) 17, doi:10.1017/S0022112006003156.

[48] F.L. Sacomano Filho, G. Kuenne, M. Chrigui, A. Sadiki, J. Janicka, A consistent artificially thickened flame approach for spray combustion using LES and the FGM chemistry reduction method: validation in Lean Partially Pre-vaporized flames, Combust. Flame 184 (2017) 68–89, doi:10.1016/j.combustflame.2017.05.031.

[49] O. Cabrit, F. Nicoud, Direct simulations for wall modeling of multicomponent reacting compressible turbulent flows, Phys. Fluids 21 (5) (2009) 1–59, doi:10.1063/1.3123528.

[50] F. Jaegle, O. Cabrit, S. Mendez, T. Poinsot, Implementation methods of wall functions in cell-vertex numerical solvers, Flow Turbul. Combust. 85 (2) (2010) 245–272, doi:10.1007/s10494-010-9276-1.

[51] F. Duchaine, S. Mendez, F. Nicoud, A. Corpron, V. Moureau, T. Poinsot, Conjugate heat transfer with large eddy simulation for gas turbine components, C.R. Mec. 337 (6–7) (2009a) 550–561, doi:10.1016/j.crme.2009.06.005.

[52] F. Duchaine, A. Corpron, L. Pons, V. Moureau, F. Nicoud, T. Poinsot, Development and assessment of a coupled strategy for conjugate heat transfer with large eddy simulation: application to a cooled turbine blade, Int. J. Heat Fluid Flow 30 (6) (2009b) 1129–1141, doi:10.1016/j.ijheatfluidflow.2009.07.004.

[53] S. Jaure, F. Duchaine, G. Staffelbach, L.Y.M. Gicquel, Massively parallel conjugate heat transfer methods relying on large eddy simulation applied to an aeronautical combustor, Comput. Sci. Discovery 6 (1) (2013) 015008, doi:10.1088/1749-4699/6/1/015008.

[54] T.J. Poinsot, S. Lele, Boundary conditions for direct simulations of compressible viscous flows, J. Comput. Phys. 101 (1) (1992) 104–129, doi:10.1016/0021-9991(92)90046-2.

[55] V. Granet, O. Vermorel, T. Léonard, L. Gicquel, T. Poinsot, Comparison of non-reflecting outlet boundary conditions for compressible solvers on unstructured grids, AIAA J. 48 (10) (2010) 2348–2364, doi:10.2514/1.J050391.

[56] L. Selle, F. Nicoud, T. Poinsot, Actual impedance of nonreflecting boundary conditions: implications for computation of resonators, AIAA J. 42 (5) (2004) 958–964, doi:10.2514/1.1883.

[57] H. Levine, J. Schwinger, On the radiation of sound from an unflanged circular pipe, Phys. Rev. 73 (4) (1948) 383–406, doi:10.1103/PhysRev.73.383.

[58] T.L. Bergman, A.S. Lavine, F.P. Incropera, D.P. Dewitt, Fundamentals of heat and mass transfer, 7th ed., John Wiley & Sons, Inc., 2011.

[59] U. Idahosa, S. Basu, A. Miglani, System level analysis of acoustically forced nonpremixed swirling flames, J. Therm. Sci. Eng. Appl. 6 (3) (2014) 031015, doi:10.1115/1.4027297.

[60] S.V. Alekseenko, V.M. Dulin, Y.S. Kozorezov, D.M. Markovich, Comparison of axial forcing effect on a strongly swirling jet and lifted propane-air flame, Proceedings of the 23th International Colloquium on the Dynamics of Explosion and Reactive Systems (2011), p. 361.

[61] J. O'Connor, T. Lieuwen, Recirculation zone dynamics of a transversely excited swirl flow and flame, Phys. Fluids 24 (7) (2012), doi:10.1063/1.4731300.

[62] M.A. Temiz, J. Tournadre, I.L. Arteaga, P. Martínez, Effect of orifice geometry on the non-linear acoustic resistance of perforated plates in the transition regime, The 22nd International Conference on Sound and Vibration: ICSV 22, 12–16 July 2015, Florence, Italy (2015a), pp. 1–8.

[63] M.A. Temiz, I. Lopez Arteaga, A. Hirschberg, Sound absorption measurements for micro-perforated plates : the effect of edge profile, Euronoise 2015, the 10th European Congress and Exposition on Noise Control Engineering, European Acoustics Association, Maastricht, The Netherlands (2015b), pp. 1–5.

[64] A. Felden, L. Esclapez, A. Misdariis, E. Riber, H. Wang, Including real fuel chemistry in large-eddy simulations, 7th European Conference for Aeronautics and Aerospace Sciences (EUCASS), Milan, Italy (2017).

[65] D. Veynante, V. Moureau, Analysis of dynamic models for large eddy simulations of turbulent premixed combustion, Combust. Flame 162 (12) (2015) 4622–4642, doi:10.1016/j.combustflame.2015.09.020.

[66] P. Wang, J. Fröhlich, U. Maas, Z. Xia He, C. Jun Wang, A detailed comparison of two sub-grid scale combustion models via large eddy simulation of the PRECCINSTA gas turbine model combustor, Combust. Flame 164 (2016) (2016) 329–345, doi:10.1016/j.combustflame.2015.11.031.